5-2016

A Risk-Based Assessment of Agricultural Water Scarcity Under Climate Change in a Semi-Arid and Snowmelt-Dominated River Basin

Hossam Moursi
Utah State University

A RISK-BASED ASSESSMENT OF AGRICULTURAL WATER SCARCITY UNDER CLIMATE CHANGE IN A SEMI-ARID AND SNOWMELT-DOMINATED RIVER BASIN

by

Hossam Moursi

A thesis submitted in partial fulfillment
of the requirements for the degree

of

MASTER OF SCIENCE

in

Civil and Environmental Engineering

Approved:

_____	_____
Jagath J. Kaluarachchi, Ph.D. Major Professor	Mac McKee, Ph.D. Committee Member
_____	_____
Thomas Lachmar, Ph.D. Committee Member	Mark R. McLellan, Ph.D. Dean of the School of Graduate Studies

UTAH STATE UNIVERSITY
Logan, Utah

2016

ABSTRACT

A Risk-Based Assessment of Agricultural Water Scarcity
Under Climate Change in a Semi-Arid and Snowmelt-
Dominated River Basin

by

Hossam Moursi, Master of Science

Utah State University, 2016

Major Professor: Dr. Jagath J. Kaluarachchi
Department: Civil and Environmental Engineering

Water scarcity is the major challenge that water managers face in semi-arid areas, especially in regions that depend on agriculture for rural livelihood. Climate change is one of the major stresses that is expected to exacerbate water scarcity problems in semi-arid regions. In this study, a risk-based approach was used to assess the climate change impacts on the risk of agricultural water scarcity in semi-arid and snowmelt-dominated river basins that are dependent on agriculture. The Sevier River Basin, located in south central Utah, was used as the case study for this work. An agricultural water deficit index was proposed to represent the basin performance in terms of water supply and agricultural water demand. The basin's natural water supply was estimated using a semi-distributed tank model. FAO AquaCrop model was used to estimate the crop water

requirements for major crops in the basin. The risk-based methodology begins using a vulnerability analysis to identify the system sensitivity to climate change. Sensitivity of system response to climatic variability was identified by establishing the climate response function, which is the relationship between basin agricultural water shortage and climate variables (i.e., precipitation and temperatures). The climate response function was then used to predict the basin agricultural water shortage in this century across four time slices using the projections of precipitation and temperature from downscaled and bias corrected GCMs outputs from the Coupled Model Intercomparison Project Phase 5 (CMIP5) for RCP4.5 and RCP8.5 scenarios.

The results of this study suggested that more natural water supply is expected in the Sevier River Basin due to the expected increase in precipitation during the future off seasons. However, projected temperature increases in the future may increase crop water requirements. It is also found that there is a high risk of unacceptable climate change impacts on agricultural water scarcity in the basin in the period 2025-2049 under RCP4.5 and for 2075-2099 under the RCP8.5 scenario, indicating climate change adaptation actions may be needed.

(55 Pages)

PUBLIC ABSTRACT

A Risk-Based Assessment of Agricultural Water Scarcity Under Climate Change in a Semi-Arid and Snowmelt-Dominated River Basin

Hossam Moursi

Water shortage is a crucial concern in the semi-arid areas that have relatively low precipitation. Given the current situation in semi-arid areas where the water supply already does not meet the water demand, climate change is one of the important factors that is expected to exacerbate the water shortage problem and make the situation even worse in the future. There are many indicators that prove climate change is happening, like the increasing land temperature, sea level rise and decreasing snow cover. Therefore, studying climate change impacts is a vital issue, especially its impacts on water resources systems.

In this research, we used a probabilistic approach to study climate change impacts on agricultural water in the Sevier River Basin, Utah. The used approach begins with identifying the basin sensitivity to climate change, and then using the projected temperature and precipitation from climate models to estimate the future agricultural water shortage.

The results of this research indicated that the Sevier River Basin system is very sensitive to precipitation and temperature changes, and consequently, to climate change.

The basin’s natural water supply is expected to increase as a result of future precipitation. In addition, the agricultural water demand is expected to increase due to rising temperature. It is indicated also that the basin will have a high risk probability of having agricultural water shortage in the period 2025-2049 and 2075-2099.

ACKNOWLEDGMENTS

I would like to thank God for his grants that he bestowed on me and for giving me the ability and power to accomplish this research.

I truly like to express my deepest gratitude and appreciation to my major advisor, Dr. Jagath J. Kaluarachchi, for advising my research and for his patience and support. No words of thanks can sum up the gratitude that I owe to Dr. Kaluarachchi for his guidance and scientific opinions which steered me in the right direction.

I would also like to thank my committee members, Dr. Mac McKee and Dr. Thomas Lachmar, for their excellent reviews and valuable feedback. Many thanks to Dr. Daeha Kim for his assistance in better understanding the Sevier River Basin system and for his cooperation in establishing the algorithm of AquaCrop and Tank models. Additional thanks to USAID for funding my academic scholarship. I acknowledge the Program for Climate Model Diagnosis and Intercomparison (PCMDI) and the WCRP's Working Group on Coupled Modeling (WGCM) for their roles in making available the WCRP CMIP5 multimodel data set.

I am very thankful to my great family in Egypt. My beloved mother, brothers and sisters, thank you so much for all you have done for me over the years. I could not have made it without your love and support. Numerous thanks to my deceased father for his great role in my life and his sacrifices for me and my family. Without the support of those all mentioned above, my thesis would not have been possible.

Hossam Moursi

CONTENTS

Page

LIST OF TABLES

Table Page

LIST OF FIGURES

Figure Page

CHAPTER 1

1. INTRODUCTION

Planning and management of water resources in semi-arid regions is a major challenge due to water scarcity. A semi-arid region is defined as a region that has an average annual precipitation of 250-600 mm/year and where evaporation is always larger than precipitation. Water scarcity happens when the water demand from all sectors (e.g., agriculture, municipal and industrial, etc.) exceeds the available water supply. Approximately, 30% of the world land area is considered arid and semi-arid and 20% of the world's population lives in these areas (Sivakumar et al. 2005). In most parts of the world, present water demand is already well in excess of supply and many more areas are expected to experience water scarcity as the world population continues to rise (Gourbesville 2008). Currently, one third of the world's population lives under high water stress and it is expected to increase to two thirds by 2025 (FAOWATER 2015).

Agricultural production plays a major role in ensuring food security. Most of the rural semi-arid areas are dependent on agricultural productivity, as 70% of the total global fresh water withdrawals are used for irrigation (Fischer et al. 2007). Therefore, the major concern for water managers of these regions is the efficient management of water use for agriculture.

While semi-arid basins already face water scarcity at the present, there are a number of factors that elevate the water shortage problem and will make the situation worse in the future. Some of the factors that may cause serious water stress in semi-arid

basins are economic growth, rapidly increasing population, high agricultural water use, groundwater depletion, and climate change.

Climate change is a top priority of these factors, which is expected to increase water scarcity and the frequency of extreme conditions, and is expected to have a serious impact on irrigated agriculture. Irrigated agriculture in arid and semi-arid watersheds is sensitive to climate change (IPCC 1995). A plenty of scientific evidences confirm that climate change is already happening and one such observation is the global warming observed during the past 100 year (IPCC 2007), as the global average surface temperature has increased by 0.74°C over the past 100 years (1906-2005). Therefore, climate change impacts on water resources systems have to be adequately addressed for sustainable water management.

Climate change impacts on water resource systems are commonly assessed by retrieving the climate information projections from general circulation models (GCMs). GCMs simulate the physical processes in ocean, land surface, and atmosphere to measure the impact of increasing concentrations of greenhouse gases on the global climate system. GCMs have significant uncertainty in simulating climate change because they do not capture the physical processes which occur at relatively fine resolution. Therefore, the potential hydrological impact of climate change plays a significant role in the uncertainties of determining the future water demand and availability (Middelkoop et al. 2001). Despite these uncertainties associated with determining the magnitude and timing of climate change impacts, water managers seek to identify these regional impacts on

their systems given the importance of climate change in water resources (Snover et al. 2003).

There are two major approaches for evaluating climate change impacts on water resources systems. The first approach is the top-down approach which is the most commonly used approach. It begins by using the climate projections of precipitation and temperature from GCMs as inputs to a hydrologic model. Since these projections typically use low spatial (100s of km) and temporal (monthly) resolution grid cells, a downscaling approach should be used to convert these results from low resolution to relatively high resolution to match the resolution of the hydrologic model. The output of the hydrologic model is then used to drive a water resource model to assess the climate risk on water resources.

This approach is popular and has been applied by many researchers, especially on evaluating the climate change impacts on irrigated agriculture (e.g., Doll 2002; Stöckle et al. 2010; Vano et al. 2010; Gondim et al. 2012; Mainuddin et al. 2014). Doll (2002) used this approach to present the first global analysis of climate change impact on irrigation requirements. Stöckle et al. (2010) studied the potential impact of climate change on the crop yield for four selected crops in eastern Washington. Vano et al. (2010) used a reservoir system model combined with a hydrologic model to study the impact of climate change on irrigated agriculture and water management in the Yakima River Basin, Washington. Gondim et al. (2012) studied the climate change impact on the irrigation water needs in the Jaguaribe River Basin in Brazil using the Hadley Centre Regional Climate Model. They used the PRECIS (Providing Regional Climates for Impacts

Studies) system to generate the climate projections using a dynamical downscaling method. Mainuddin et al. (2014) studied the climate change impact on the irrigation requirements for the main crops in Bangladesh using a soil water balance simulation model (SWB).

The limitation of this approach is that it increases the uncertainty associated with evaluating the climate change impacts, because every climate model and a corresponding emission scenario gives different results. In addition, this approach typically uses a small selection of climate models and scenarios because of the computational burdens for downscaling the GCM results and simulating the hydrologic model for each climate model and scenario combination. As a result, this approach does not capture the full range of future climate conditions (García et al. 2015). Therefore, a probabilistic approach could be more appropriate for assessing the climate change impacts to fully analyze and capture the uncertainty associated with different GCMs and emission scenarios.

An alternative approach is the bottom-up decision-scaling methodology described by Brown et al. (2012). It integrates a bottom-up stochastic analysis to assess the system vulnerability with top-down use of GCM projections to estimate the relative probability of a future climate hazard. This approach consists of three steps. The first step is the characterization of the system and its performance indicators (e.g., system reliability) and identification of the threshold of acceptable performance that does not need a remedial action and unacceptable system performance that requires a further action. The second step is using a stochastic analysis to establish the climate response function to identify the

system climate sensitivity. The climate response function is the relationship between the system performance indicator and the climate variables. The third step is using different datasets of GCM runs to estimate the future values of the system performance indicator. Then the relative probability of each climate state of the acceptable and unacceptable performance can be estimated.

The advantage of this approach is that it can use a large number of GCM projections and scenarios without conducting the analysis for each projection dataset. It can capture the full possible range of GCMs outputs and reduces the associated uncertainty in assessing the climate change impact while minimizing the computational effort. This approach is innovative and Brown et al. (2012) applied it to a simple municipal surface water supply system that included a supply reservoir. Ghile et al. (2014) used the decision-scaling approach to assess the climate change impact on infrastructure investment in the Niger River Basin. Li et al. (2014) demonstrated the same approach in the analysis of climate change impacts on a large water supply system in Massachusetts, USA.

An example of rural semi-arid basins that is dependent on agricultural economy is the Sevier River Basin in Utah. It is located in south central Utah in the southwestern United States, which is considered the most arid region in the US, and is expected to face more water scarcity and more intense and frequent droughts (Seager et al. 2007). In addition, the basin water supply is driven from snowmelt, as winter precipitation is stored in the snowpack and discharged in the water demand season. Approximately 70-80% of the total runoff in the mountainous regions of the western US is derived from snowmelt

(Doesken and Judson 1997). Since climate change is expected to decrease snowpack accumulation and cause earlier snowmelt runoff, reduced water availability can cause serious water shortages during the growing season in these snowmelt-dominated regions (Llewellyn and Vaddey 2013).

In this research, we extended the methodology proposed by Brown et al. (2012) to assess the climate change impact on agricultural water scarcity in the Sevier River Basin. The Sevier River Basin, Utah is used as the test case for this demonstration.

This thesis is structured into 5 chapters where Chapter 1 is the introduction. Chapter 2 contains a description of the Sevier River Basin study area and the data used in this research. Chapter 3 describes the research methodology and the simulation models used. Chapter 4 presents the research results and discussion. Chapter 5 provides the research summary and conclusions.

CHAPTER 2

2. STUDY AREA AND DATA

2.1 Description of Study Area

The study area is the Sevier River Basin located in south-central Utah (Figure 1). It encompasses approximately an area of 27,389 km^2 (12.5% of Utah's area) with a relatively high evapotranspiration (ET) and low precipitation, and is characterized as snowmelt-driven streamflows due to high elevation. The mean annual precipitation ranges between 250 and 1000 mm along the elevation profile. Particularly, water from the Sevier River has been highly regulated for irrigating farm lands, developed along the main channel and its tributaries, mainly by three reservoirs (Piute, Otter Creek, and Sevier Bridge Reservoirs). Most of the water supply from the reservoirs is used for agricultural production for rural livelihood; thus, decreasing snowfall and early spring runoff are important challenges for efficient water management, especially under climate change. Major irrigated crops are pasture and grass hay (45%), alfalfa (44%), maize (6%), barley (4%), and wheat (1%). Productivity of crops is significantly dependent on water availability from the three reservoirs during the growing season, which is from April to September. There exist municipal and industrial water demands, but these demands are small in comparison to the dominant agricultural water demand.

In the Sevier River Basin, streamflows mostly originate from the upper watersheds in higher elevations, but water is consumed mostly by farm lands in the lower elevations given the higher water right according to the prior appropriation doctrine of

the western USA. Hence, farm lands near Delta have well supplied water from storage in the reservoirs. Farm lands near Fillmore are outside the geologic boundaries of the Sevier River Basin, but are irrigated by surface water from the Sevier River transported via the Central Utah Canal, as well as local groundwater sources.

For the climate change impact assessment, the upper basin above the Sevier Bridge Reservoir is divided into 23 watersheds for simulating streamflows that account for most of the natural water supply to the reservoirs. Runoff from watersheds below the Sevier Bridge Reservoir is neglected due to high ET losses. To estimate the agricultural water demands, the farm lands along the main channel and tributaries are represented by eight regions: Delta, Oak, Ephraim, Fillmore, Richfield, Angle, Circleville and Panguitch, as shown in Figure 1.

2.2 Climate and Soil Data

We used daily precipitation, and maximum and minimum temperatures from 1994 to 2015 (22 years) at 12 Snow Telemetry (SNOTEL) stations operated by the U.S. Department of Agriculture (USDA) for simulating natural flows in the 23 watersheds (available at http://www.wcc.nrcs.usda.gov/snow/). We additionally collected daily precipitation and temperatures with the same length from the National Climatic Data Center (NCDC; available at http://www.ncdc.noaa.gov/) of the National Oceanic and Atmospheric Administration (NOAA) for estimating irrigation requirement using AquaCrop in the eight farming regions. The number of NOAA stations used in this study was six. In total, 18 climatic stations located across the Sevier River Basin were used for

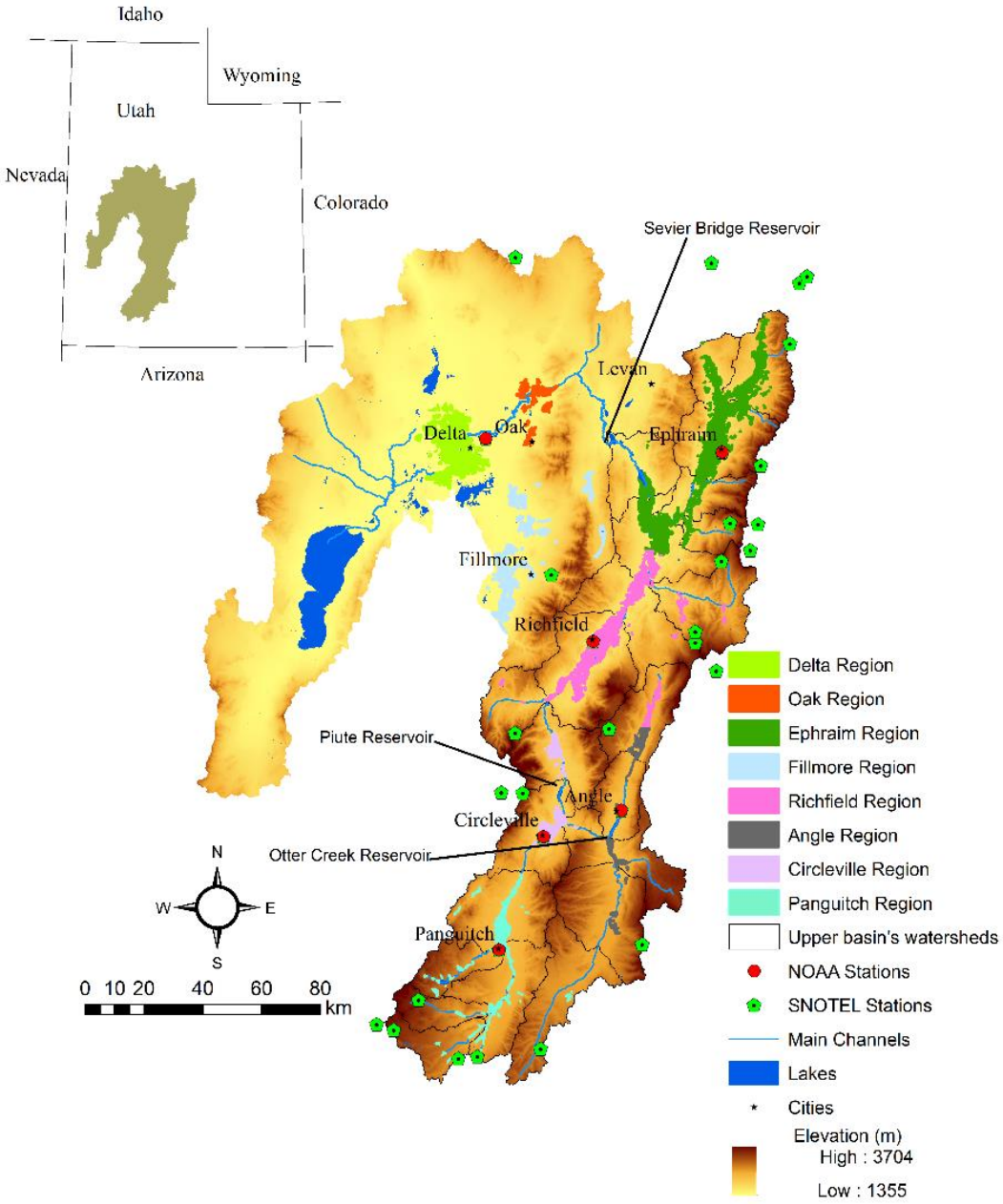

Figure 1. Physical layout of the Sevier River Basin, Utah.

this study, and are listed along with their corresponding watersheds and farming regions in Table 1. However, for generating the 10,000 year stochastic simulations, we used the data form the total 31 stations located in the basin to preserve the spatial correlations between them. Due to the absence of wind speed and relative humidity data with the same length of precipitation and temperature datasets, we used a constant wind speed obtained from nearby USDA Soil Climate Analysis Network (SCAN) stations and minimum temperatures for estimating reference ET in the eight farming regions.

The soil physical properties required for estimating irrigation water requirement using AquaCrop are saturated hydraulic conductivity (K_{sat}), saturated water content (Θ_{sat}), field capacity (Θ_{fc}), bulk density (BD), permanent wilting point (Θ_{wp}) and electrical conductivity (EC). These data were obtained from SSURGO (Soil Survey Geographic Database) and STATSGO2 (State Soil Geographic Database) provided by the USDA Natural Resources Conservation Service. For estimating cropping area and crop classification, we used the CropScape data of USDA given at 30×30 m^2 spatial resolution. The area of the five major crops in the basin in each farming region and the soil properties of each farming region are shown in Table 2. It should be noted that we refer to the crop areas here as crops that are irrigated from surface water supply only. We estimated the crop areas that are irrigated from groundwater supply by multiplying the total crops area by the percent of groundwater use; and subtracted it from the total crop area.

Table 1. Details of SNOTEL and NOAA stations located in different sub-watersheds and farming regions in the Sevier River Basin.

Sub-watershed	SNOTEL Station	Farming Region	NOAA Station
Asay Creek	Midway Valley	Delta	Delta
Mammoth Creek	Castle Valley	Oak	Delta
Panguitch Creek	CastleValley	Ephraim	Ephraim USFS
Pass Creek Sevier River	Long Valley JCT	Fillmore	Delta
Bear Creek Sevier River	Big Flat	Richfield	Richfield Radio KSVC
City Creek Sevier River	Big Flat	Angle	Angle
Upper East Fork Sevier River	Agua Canyon	Circleville	Circleville
Middle East Fork Sevier River	Widtsoe 3	Panguitch	Panguitch
Lower East Fork Sevier River	Widtsoe 3		
Upper Otter Creek	Box Creek		
Lower Otter Creek	Box Creek		
Beaver Creek Sevier River	Kimberly Mine		
Clear Creek	Kimberly Mine		
Cottonwood Creek Sevier River	Box Creek		
Lost Creek Sevier River	Farnsworth Lake		
Salina Creek	Pickle KEG		
Willow Creek	Pickle KEG		
Silver Creek	Mammoth Cottonwood		
Upper San Pitch River	Mammoth Cottonwood		
Middle San Pitch River	Seeley Creek		
Lower San Pitch River	Seeley Creek		
Twelvemile Creek	Beaver Dams		
Sevier Bridge	Beaver Dams		

Table 2. Irrigated crop areas and soil properties for each farming region in the Sevier River Basin.

	Delta	Ephraim	Circleville	Panguitch	Angle	Richfield	Fillmore	Oak
Crop Area (acres)								
Barley	2415	2751	292	31	349	1565	368	153
Wheat	750	568	14	14	8	127	825	303
Corn	2161	3716	379	204	73	4098	1680	481
Alfalfa	11730	33659	6171	5144	3563	21338	10613	3750
Pasture	1747	49736	6859	14099	6341	18507	1184	298
Soil properties								
K_{sat} (mm/day)	584	1590	1930	2110	2789	2987	1163	1566
Θ_{fc}	0.24	0.24	0.20	0.20	0.17	0.23	0.21	0.20
Θ_{wp}	0.12	0.12	0.10	0.10	0.08	0.12	0.11	0.10
BD (gm/cm^3)	1.30	1.25	1.31	1.35	1.37	1.25	1.31	1.32
Θ_{sat}	0.51	0.53	0.51	0.49	0.48	0.53	0.51	0.50
EC (ds/m)	13.5	5.2	0.9	1.7	1.4	4.5	3.9	4.9

CHAPTER 3

3. METHODOLOGY

3.1 Proposed Framework for Climate Change Impact Assessment

For assessing climate change impacts on basin-wide agricultural water scarcity, we adopted the decision-scaling approach proposed by Brown et al. (2012). While a typical climate change impact assessment uses GCMs as inputs of system models (e.g., runoff or crop models), the decision-scaling approach evaluates system sensitivity to climatic variability first and provides the degree of climate change with respect to the system sensitivity. If climate is not sensitive to the system behavior or specific system performance outputs, then further action may not be needed. In the case of high climate sensitivity, then the analysis is continued to assess the actual relevant climate change impacts. The proposed approach consists of three steps, which are shown in Figure 2.

The first step is to identify the system models and corresponding performance indicators together with one or multiple thresholds of acceptable performance. The system models used in this study are the semi-distributed Tank Model similar to the work Cooper et al. (2007) for estimating natural water supply, and FAO AquaCrop (Steduto 2009), and the approach of Masoner et al. (2003) for estimating irrigation water requirements. Agricultural water deficit is the major concern for water managers in the Sevier River Basin, since the largest portion of water is used for irrigation purposes. Therefore, an annual agricultural water deficit index (I_t) is defined as the system performance indicator. I_t is defined using annual water availability (S_t) and agricultural

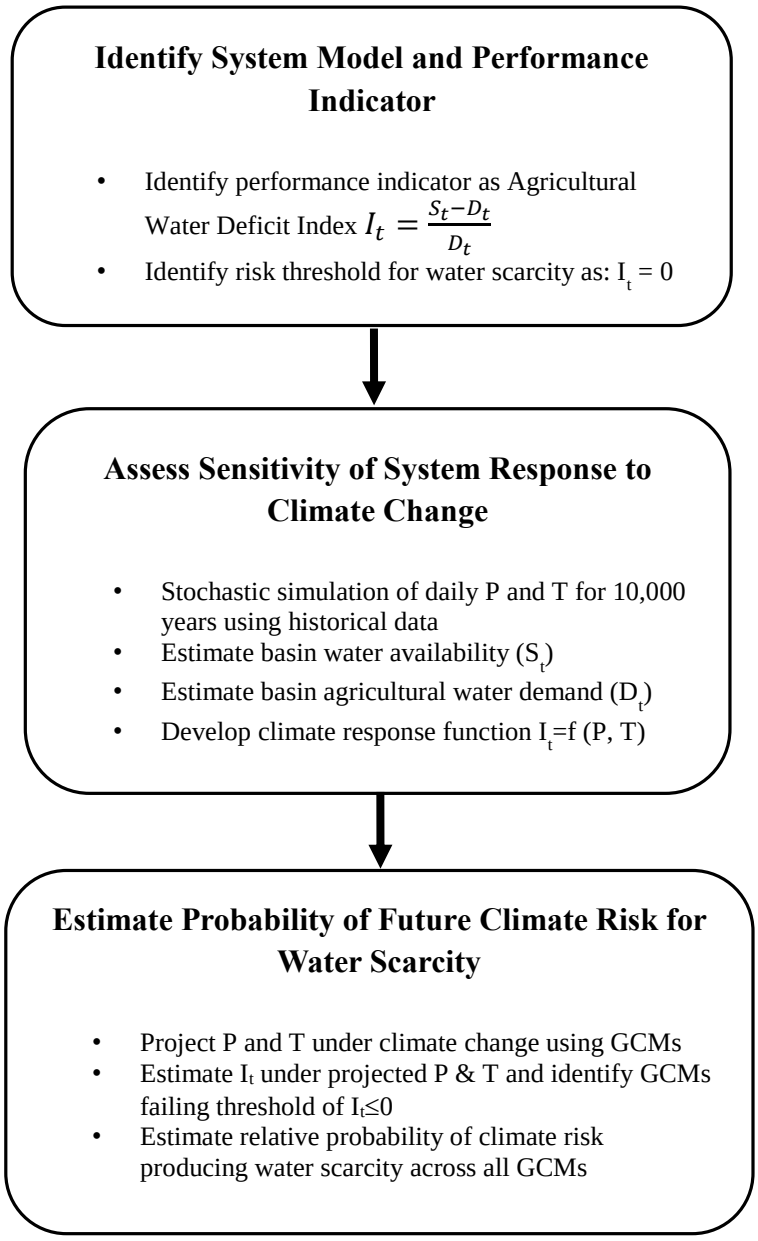

Figure 2. Flow chart illustrating the proposed methodology for climate risk assessment, where P and T are basin precipitation and temperature, respectively.

water demand (D_t):

$$I_t = \frac{S_t - D_t}{D_t} \quad (1)$$

where, S_t is total annual volume of streamflow in year (t) estimated by the semi-distributed Tank Model (Mm^3), and D_t is total volume of seasonal irrigation water required (Mm^3) for attainable crop yields simulated by AquaCrop and the approach of Masoner et al. (2003). Attainable crop yield is defined here as the yield that can be reached under good water management practices. More details of this definition will appear later. A higher I_t value indicates a lower agricultural water shortage and vice versa. When I_t is equal to or greater than zero, no agricultural water deficit exists (i.e. natural water supply meets the agricultural demand). Therefore, we defined the threshold of the acceptable basin performance as $I_t = 0$.

The second step is to identify the sensitivity of system response to climatic variability by sampling a broad range of possible climate change scenarios using a stochastic simulation. To accommodate a broad sampling range of climatic conditions, we first extended the relatively short climatic data (i.e. 22-year precipitation and temperatures) to 10,000 years using multi-site stochastic models. S_t and D_t are simulated using stochastically generated 10,000-year precipitation and temperatures as inputs to the system models, and therefore I_t values for 10,000 years are computed from the system models. Using these I_t values and annual precipitation and temperature values, a relationship between I_t and climate conditions, temperature and precipitation, can be established. This relationship is typically called the climate response function.

In step 3, multiple GCMs are used as inputs to the climate response function to estimate the future probability distribution of agricultural water deficit index. The climate response function provides the ease of including multiple GCMs in the analysis. Once the climate response function is established, no additional simulation using the system models is necessary. Hence, agricultural water scarcity corresponding to a GCM can be quickly found using the climate response function. By assessing the effects of multiple GCMs to the climate response function, the limitation of selecting one to few GCMs, which is a major drawback of typical climate change impact assessments, can be reduced. Descriptions of the stochastic model and basin models are in the following sections.

3.2 Stochastic Generation of Climatic Observations

The Markov chain model and the first-order vector autoregressive (VAR1) model for multiple sites formulated by Wilks (1999) are used for the 10,000-year generation of precipitation and temperature. Previous results showed good performance in reproducing mean, variance, and spatial correlation of observations at 62 stations located in Oregon and Idaho, and the methodology has been widely used for various purposes, including the basis of many weather generation studies (e.g., Qian et al. 2002; Brissette et al. 2007; Srikanthan and Pegram 2009; Keller et al. 2015).

The precipitation model uses the first-order Markov chain and the mixed exponential distribution for occurrence and amount of precipitation, respectively. To reproduce observed spatial correlations between gauging stations, Wilks (1999) incorporated multivariate Gaussian random numbers into the Markov Chain model. The

correlation matrix of the multivariate Gaussian distribution is obtained by observed spatial correlations and a generic regression with an exponential function and distances between gauging stations. Besides, the analytical solution of the VAR1 model is used for generating temperatures. The time-series of daily maximum and minimum temperatures are standardized with single-wave cosine functions for each station. Dry and wet days are separately standardized using precipitation generated by the Markov-chain model to stipulate lower averages on wet days. Although a matrix adjustment was necessary for the analytical parameter estimation in the case of 62 stations in the original study of Wilks (1999), the 31 stations of this study did not require the adjustment process. Further details of the multi-site daily weather generation model are found in Wilks (1999).

3.3 Estimation of Annual Water Supply

For simulating natural flows from 23 watersheds, we used the semi-distributed tank model proposed by Kim and Kaluarachchi (2014) that includes SNOW-17 of the National Weather Service (Anderson 1976) to simulate the snowmelt process. SNOW-17 has 12 parameters (5 for snowmelt, 7 for runoff) and uses daily precipitation, and maximum and minimum temperatures as inputs. It divides a watershed into five zones with the elevation profile, and thus considers the effects of elevation on precipitation and temperatures. The runoff component (i.e., watershed response to rainfall and snowmelt) of the model is conceptualized by a two-layer tank proposed by Cooper et al. (2007). Kim and Kaluarachchi (2014) calibrated the semi-distributed tank model for 13 gauged

watersheds in or adjacent to the Sevier River Basin using a genetic algorithm, and found consistent performance for simulating natural flows across the upper Sevier River Basin.

For estimating annual water supply, we used the proximity-based regionalization approach for 23 watersheds in this study. In other words, the calibrated parameter sets of 13 gauged watersheds in Kim and Kaluarachchi (2014) were transferred to the 23 watersheds of this study based on proximity. Hence, the streamflow in each watershed was simulated using the 10,000-year precipitation and temperature values and transferred parameter sets. The simulated streamflows from the 23 watersheds were finally summed up for representing the basin-wide natural water supply.

3.4 Estimation of Irrigation Water Requirements

FAO AquaCrop (Steduto et al. 2009) was used to estimate the water requirements for major crops (alfalfa, maize, barley, and wheat) in the eight farming regions. FAO AquaCrop has been frequently used and provided reliable estimates of water requirements for major crops in prior studies (e.g., Araya et al. 2010; Stricevic et al. 2011; Vanuytrecht et al. 2014) based on its simplicity and robustness. It simulates crop yield response to water and salinity on a daily basis, and provides yield estimates per a given irrigation management schedule. Iterative simulations with changing irrigation schedules provide seasonal water requirement and corresponding attainable crop yield. Kim and Kaluarachchi (2015, 2016) calibrated the parameter sets for the target crops in farm lands near Delta using Landsat images and regional crop information. We used these calibrated parameter sets for the eight farming regions of this study.

For estimating basin-wide agricultural water demand, we first determined the best irrigation schedule by testing 10 irrigation intervals (3-30 days with steps of 3 days) per seasonal irrigation depth. The maximum yields among the 10 schedules is considered to be the yield at the given seasonal irrigation depth. We assumed the crop yield at 1,500 mm of seasonal irrigation depth is the attainable yield, and determined the required irrigation depth for each crop at which the simulated yield becomes 95% of the attainable yield (Figure 3).

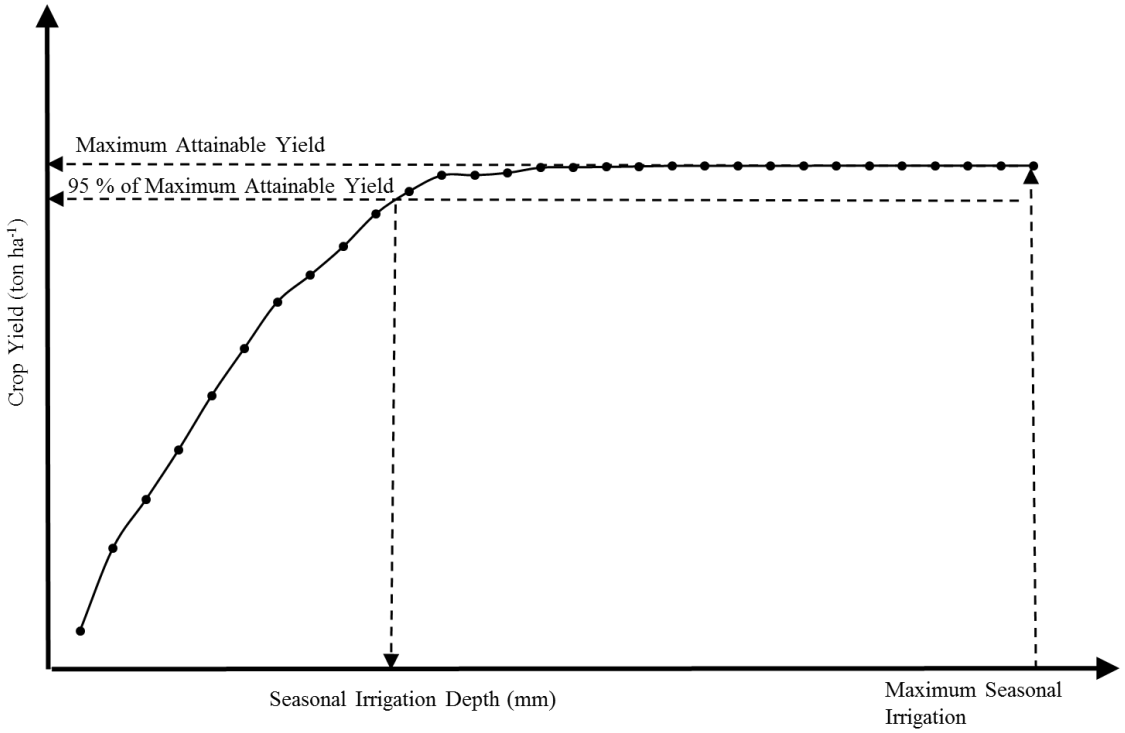

Figure 3. A graph illustrating the algorithm for calculating the agricultural water requirement in AquaCrop.

The agricultural water demand for each crop in each farming region was estimated by multiplying the simulated irrigation requirements and planting areas. Seasonal

irrigation requirements for pasture and grass hay, which are unavailable in AquaCrop, were estimated using the approach of Masoner et al. (2003), and included as an additional water demand. The basin-wide agricultural water demand is obtained by summing up all demands in the eight farming regions. Because this complex simulation is very time-consuming when using all 10,000-year climatic inputs in AquaCrop, we simulated agricultural water demand for 100-year inputs first and developed a regression model between agricultural water demand and climatic conditions. The 10,000-year agricultural water demands are estimated by the regression model:

$$D_t = 1158 - 0.5721 * P_c - 2.771 * 10^5 * T_{cmax}{}^{-2} \ (R^2 = 0.75) \qquad (2)$$

where D_t is annual agricultural water demand (Mm^3), t is time (years), P_c and T_{cmax} are total precipitation (mm) and maximum temperature (°C) during the growing season (April to September), respectively.

3.5 GCMs and Downscaling Methods

The projections of precipitation and temperatures were obtained from GCMs from the coupled model intercomparison project phase 5 (CMIP5). The projections were bias corrected and used statistically downscaled datasets as described by Maurer et al. (2007) for the period 2000-2099. Two Representative Concentration Pathways (RCPs), RCP4.5 and RCP8.5, were used to accommodate both intermediate and very high greenhouse gas concentrations, respectively., RCP4.5 and RCP8.5 emission scenarios are commonly used in many climate change assessment studies (e.g., Yan et al. 2015, He et al. 2015 and

Zhang 2016). The labels 4.5 and 8.5 refer to the expected anomaly in radiative forcing in watt/m^2 by year 2100.

As reported in the IPCC 2013 report, RCP4.5 is characterized by stabilizing the greenhouse gases concentration after year 2100, and the emissions peak occurs around year 2040 and declines thereafter. It assumes a medium population growth, higher rate of technology development, cropland area decrease, and emission mitigation policy to decrease the fossil fuel use. The average global temperature in RCP4.5 is projected to increase by 1.1 to 2.6 °C and the global sea level is projected to increase by 0.32 to 0.63 m, relative to the 1986-2005 average.

While, RCP8.5 is characterized by increasing the green gas concentration over time with continued increase after 2100. It assumes a high population growth, lower rate of technology development, cropland area increase, and the global use about 80% of energy from fossil fuels. The average global temperature in RCP4.5 is projected to increase by 2.6 to 4.8 °C and the global sea level is projected to increase by 0.45 to 0.82 m, relative to 1986-2005 average.

In this study, the numbers of GCMs used for RCP4.5 and RCP8.5were 31 and 29 respectively. The climate models used for each scenario and the information for each model are provided in Table 3. These projections were used to project the future basin agricultural water shortage under the climate change.

Table 3. Information of 31 and 29 GCMs used in the analysis for RCP4.5 and RCP8.5 scenarios respectively, with NA indicating non-availability. Adapted from Program for Climate Models Diagnosis and Intercomparison (PCMDI).

GCM	Emission Path		Institution
	RCP4.5	RCP8.5	
ACCESS1.0	*	*	CSIRO (Commonwealth Scientific and Industrial Research Organisation, Australia), and BOM (Bureau of Meteorology, Australia)
BCC-CSM1.1	*	*	Beijing Climate Center, China Meteorological Administration
BCC-CSM1.1(M)	*	*	Beijing Climate Center, China Meteorological Administration
CANESM2	*	*	Canadian Centre for Climate Modelling and Analysis
CCSM4	*	*	National Center for Atmospheric Research
CESM1-BGC	*	*	National Science Foundation, Department of Energy, National Center for Atmospheric Research
CESM1-CAM5	*	*	National Science Foundation, Department of Energy, National Center for Atmospheric Research
CMCC-CM	*	*	Centro Euro-Mediterraneo per I Cambiamenti Climatici
CNRM-CM5	*	*	Centre National de Recherches Meteorologiques / Centre Europeen de Recherche et Formation Avancees en Calcul Scientifique
CSIRO-MK3.6.0	*	*	Commonwealth Scientific and Industrial Research Organisation in collaboration with the Queensland Climate Change Centre of Excellence
FGOALS-G2	*	*	LASG, Institute of Atmospheric Physics, Chinese Academy of Sciences; and CESS, Tsinghua University
FIO-ESM	*	*	The First Institute of Oceanography, SOA, China
GFDL-CM3	*	*	Geophysical Fluid Dynamics Laboratory
GFDL-ESM2G	*	*	Geophysical Fluid Dynamics Laboratory
GFDL-ESM2M	*	*	Geophysical Fluid Dynamics Laboratory

Table 3 (Continued).

GCM	Emission Path		Institution
	RCP4.5	RCP8.5	
GISS-E2-H-CC	*	NA	NASA Goddard Institute for Space Studies
GISS-E2-R	*	*	NASA Goddard Institute for Space Studies
GISS-E2-R-CC	*	NA	NASA Goddard Institute for Space Studies
HADGEM2-AO	*	*	National Institute of Meteorological Research/Korea Meteorological Administration
HADGEM2-CC	*	*	Met Office Hadley Centre
HADGEM2-ES	*	*	Met Office Hadley Centre and Instituto Nacional de Pesquisas Espaciais
INM-CM4	*	*	Institute for Numerical Mathematics
IPSL-CM5A-MR	*	*	Institut Pierre-Simon Laplace
IPSL-CM5B-LR	*	*	Institut Pierre-Simon Laplace
MIROC-ESM	*	*	Japan Agency for Marine-Earth Science and Technology, Atmosphere and Ocean Research Institute (The University of Tokyo), and National Institute for Environmental Studies
MIROC-ESM-CHEM	*	*	Japan Agency for Marine-Earth Science and Technology, Atmosphere and Ocean Research Institute (The University of Tokyo), and National Institute for Environmental Studies
MIROC5	*	*	Atmosphere and Ocean Research Institute (The University of Tokyo), National Institute for Environmental Studies, and Japan Agency for Marine-Earth Science and Technology
MPI-ESM-LR	*	*	Max Planck Institute for Meteorology (MPI-M)
MPI-ESM-MR	*	*	Max Planck Institute for Meteorology (MPI-M)
MRI-CGCM3	*	*	Meteorological Research Institute
NORESM1-M	*	*	Norwegian Climate Centre

CHAPTER 4

4. RESULTS AND DISCUSSION

4.1 Climate Response Function

The 10,000-year stochastically generated precipitation and temperature profiles were used to estimate basin-wide annual water availability (S_t) and agricultural water demand (D_t). A multiple regression model was used to establish the climate response function (i.e. the relationship between I_t and representative precipitation and temperatures) as shown in Equation (3) with a R^2 of 0.73.

$$\log(I_t + 1.8) = -0.8029 + 0.001351 * P_c + 0.003472 * P_o + 105.5 * {T_{cmax}}^{-2} \quad (3)$$

where, P_c and T_{cmax} are total precipitation (mm) and maximum temperature (°C) during the growing season (April to September), respectively, and P_o is total precipitation (mm) during off-season (October to March). All independent variables were significant (p-values << 0.001), and the regression model showed no multicollinearity based on its variance inflation factor of less than 2.

The climate response function indicates that higher precipitation and lower maximum temperature during a growing season result in less basin-wide agricultural water demand. This is because higher rainfall and lower temperature reduces irrigation water requirement for attainable yields. Off-season precipitation is mostly snowfall that becomes natural water supply in the upcoming growing season, and therefore it is highly sensitive to off-season precipitation. Based on the climate response function, the system is more sensitive to off-season precipitation change than precipitation during the growing

season. An increase of 5% in P_o would result in an increase of I_t by 46%, while the same change in P_c increases I_t by only 14%. An increase of 1°C in T_{cmax} would decrease I_t by 17%. Overall, P_o is the most important parameter affecting basin-wide agricultural water scarcity, and T_{cmax} and P_c are the next most important parameters.

4.2 Climate Change Impacts

The projected precipitation and temperature from GCMs were used to estimate I_t and statistically analyzed for four periods: 2000-2024, 2025-2049, 2050-2074 and 2075-2099 with scenarios RCP4.5 and RCP8.5. Each period has 25 values of I_t. In general, RCP4.5 and RCP8.5 scenarios show an increase in annual precipitation and temperature. Table 4 shows the percent of change of precipitation and temperature for the four time periods: 2000-2024, 2025-2049, 2050-2074 and 2075-2099 for both scenarios RCP4.5 and RCP8.5. Both scenario projections have an increasing trend in P_o and T_{cmax}. The annual mean temperature rises according to both scenarios by 2.5 ◦C and 4.9 ◦C under RCP4.5 and RCP8.5, respectively at the end of 21st century. P_c has a decreasing trend under RCP8.5 but it does not have a similar consensus under RCP4.5. Figures 4 through 6 show the changes in the three variables of the climate response function: P_o, P_c, and T_{cmax} respectively, under the RCP4.5 scenario. These findings are consistent with the projections of precipitation and temperature estimates from previous studies (e.g., Christensen and Lettenmaier 2006). Christensen and Lettenmaier (2006) found that the mean temperature in Colorado River Basin will increase in the period 2070-2099 by 2.7

and 4.4 ^{0}C for less and high emissions scenarios, respectively. They also found that winter precipitation will increase.

Table 4. Percent change in future precipitation and temperature for RCP4.5 and RCP8.5 scenarios. dP_c and dP_o are the percent changes in growing season precipitation and off-season precipitation, respectively. dT_{cmax} and dT are the changes in maximum temperature during the growing season and annual average temperature, respectively.

Scenario	Parameter	2000-2024	2025-2049	2050-2074	2075-2099
RCP4.5	dP_c (%)	6.9	5.6	9.0	6.8
	dP_o (%)	-2.7	-0.8	0.9	4.1
	dT_{cmax} (^{0}C)	2.4	3.5	4.2	4.7
	dT(^{0}C)	0.3	1.3	2.1	2.5
RCP8.5	dP_c (%)	7.1	6.0	5.4	2.0
	dP_o (%)	-2.0	2.9	5.5	10.5
	dT_{cmax} (^{0}C)	2.5	3.8	5.5	7.4
	dT (^{0}C)	0.4	1.7	3.3	4.9

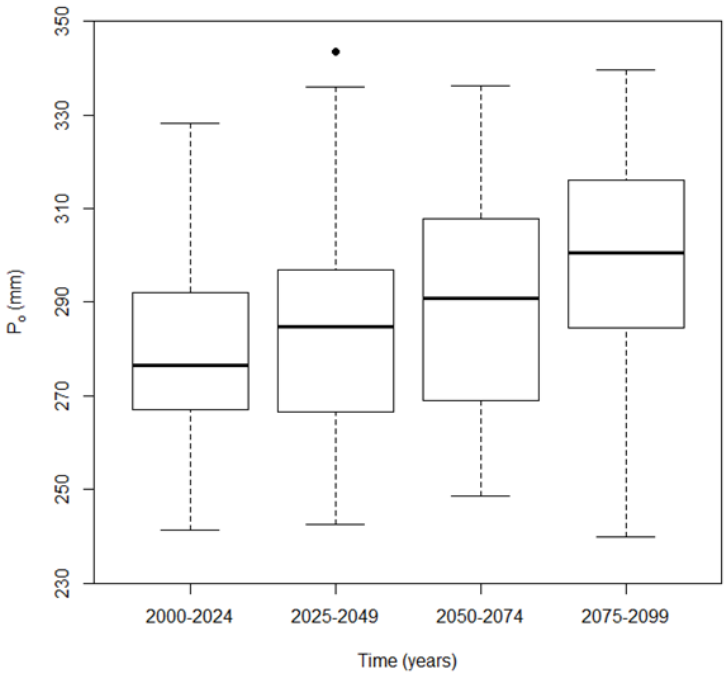

Figure 4. Projections of precipitation during the off-season (P_o) for the RCP4.5 scenario.

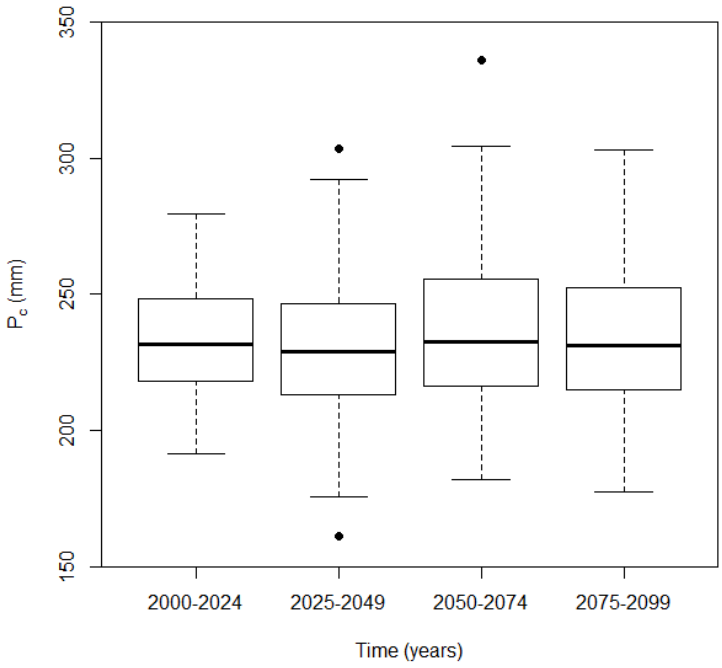

Figure 5. Projections of precipitation during the growing season (P_c) for the RCP4.5 scenario.

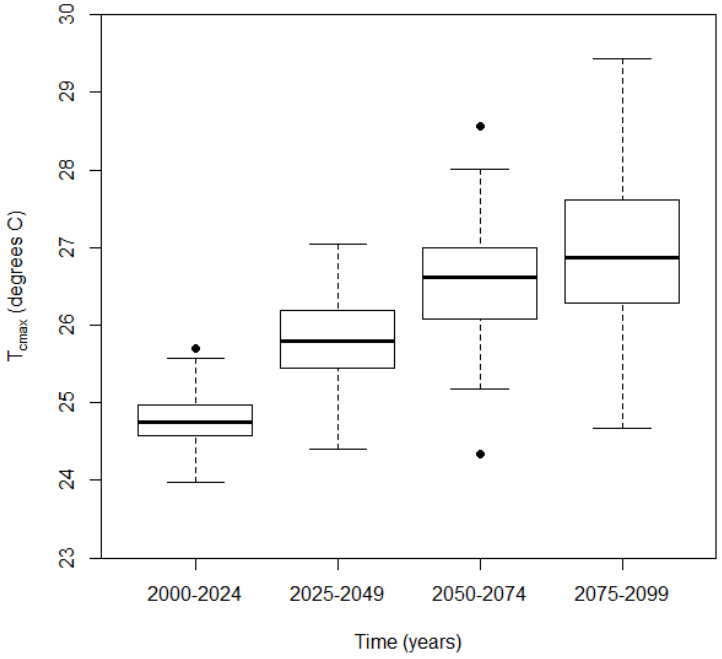

Figure 6. Projections of maximum temperature during the growing season (T_{cmax}) for the RCP4.5 scenario.

Figure 7 shows the estimated box plots of I_t values obtained from the GCMs under RCP4.5 with similar results for RCP8.5 in Figure 8. Although all time periods have GCMs with negative I_t values for both scenarios, mean values indicate no water scarcity even under changing climate. Indeed, there is an increasing trend in the average of I_t values, and this is because of increasing P_o under both scenarios. Greater I_t values were obtained under RCP8.5 than RCP4.5 due to higher P_o values with RCP8.5. From the results, it is evident that more natural water supply can be expected in the Sevier River Basin due to increasing off-season precipitation, but rising maximum temperature during growing season can increase higher irrigation requirements as well.

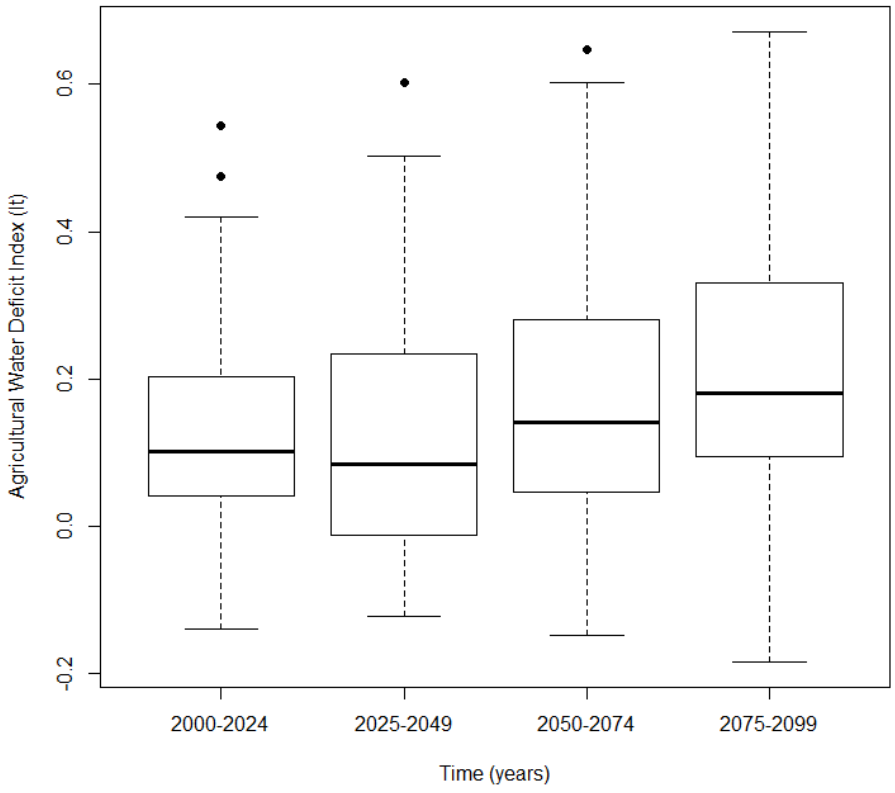

Figure 7. Box plot of future agricultural water deficit index (I_t) predicted by GCM projections for RCP4.5.

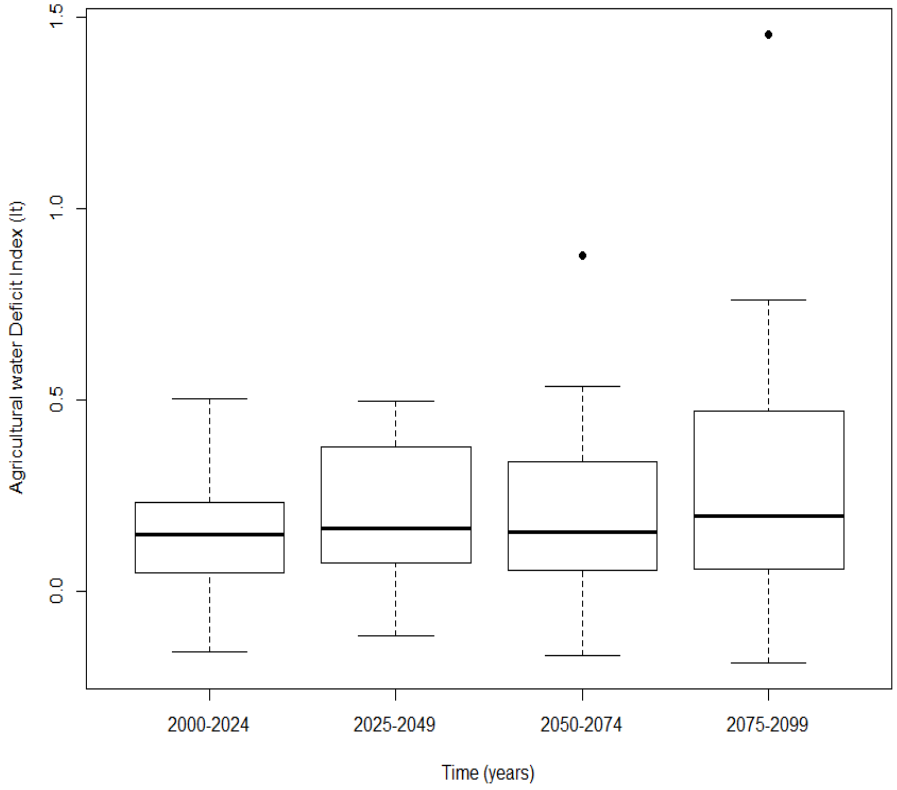

Figure 8. Box plot of future agricultural water deficit index (I_t) predicted by GCM projections for RCP8.5.

One advantage of the climate response function is to identify the climatic conditions affecting water availability through values below the threshold ($I_t < 0$). Since the climate response function has three predictor variables (see Equation 3), it is not possible to provide a single plot. Instead plots were made with two variable while keep the third one constant. Figure 9 shows the plot with constant off-season precipitation (P_o), while Figure 10 shows the same with constant growing season precipitation (P_c). In Figure 9, the points are the average of growing season maximum temperature and precipitation over the period 2000-2099 for the 31 and 29 GCMs from the RCP4.5 and RCP8.5 scenarios, respectively. Similarly, the points in Figure 10 are the average of

growing season maximum temperature and off-season precipitation. GCM projections from both scenarios are imposed with the contour lines of the agriculture water deficit index to identify the GCMs that have unacceptable thresholds ($I_t < 0$). There are number of GCM projections in both scenarios that are below the threshold ($I_t < 0$), which are to the left to the zero contour line. These climatic conditions are problematic and have the potential of producing water scarcity or climate risk in the different time periods. As shown in Figure 9, there are 1 out of 31 GCMs for RCP4.5 and 2 out of 29 GCMs for RCP 8.5 that produce climate risk. Similarly, in Figure 10, there are 4 out of 31 GCMs for RCP4.5 and 6 out of 29 GCMs for RCP8.5 that produce climate risk. In general, it can be stated that the results indicate lower probability of climate risk for water scarcity with both emission scenarios.

After estimating the agricultural water deficit index, the values are compared with the threshold ($I_t=0$) to calculate the probability of exceeding the threshold. The cumulative probability of climate conditions was estimated by using a nonparametric empirical distribution presented by Wilks 1995, as shown in Equation 4. The cumulative probability of X variable is the probability that X will take a value less than or equal to x. Each GCM run is assumed to have an equal probability of occurrence in the future.

$$P = \frac{m}{n+1} \qquad (4)$$

where P is cumulative probability, m is rank of data, and n is the total number of data values.

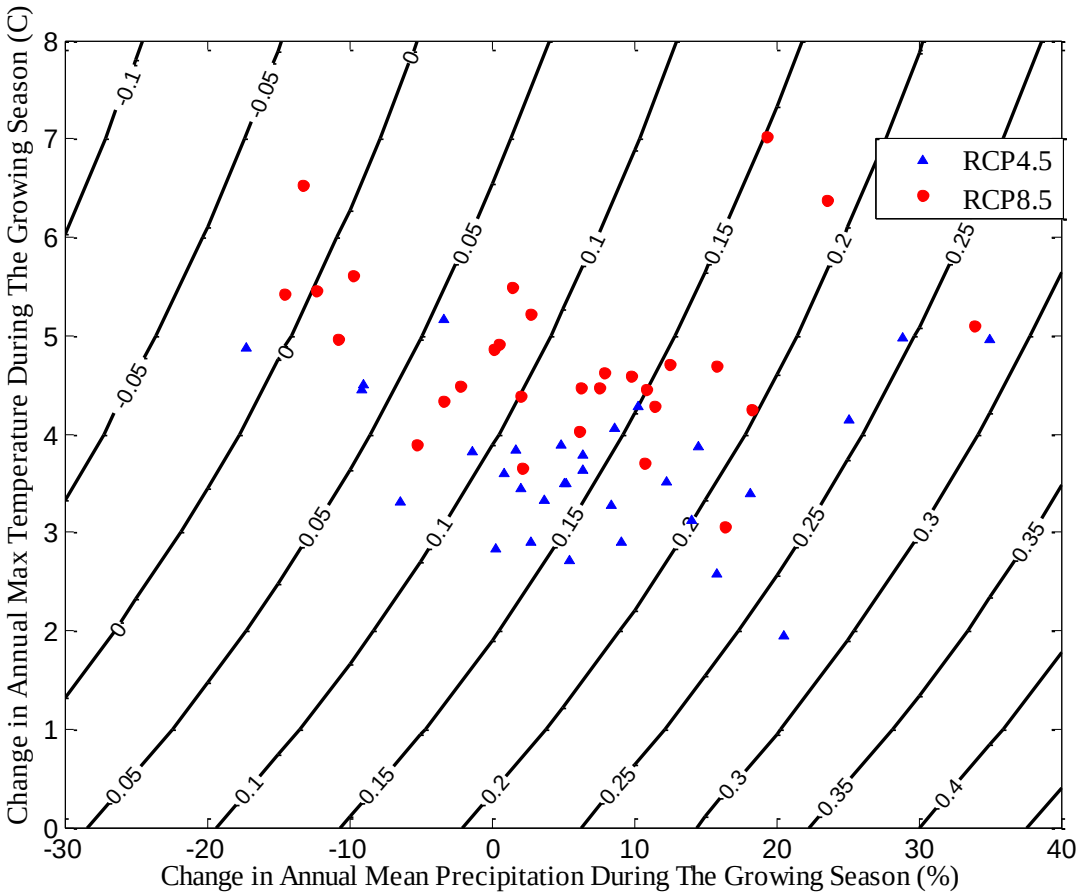

Figure 9. Scatterplot of % change in annual mean precipitation and annual maximum temperature during the growing season, superimposed on the contour lines of I_t for RCP4.5 and RCP8.5 scenarios when P_o is constant at 286.7 mm.

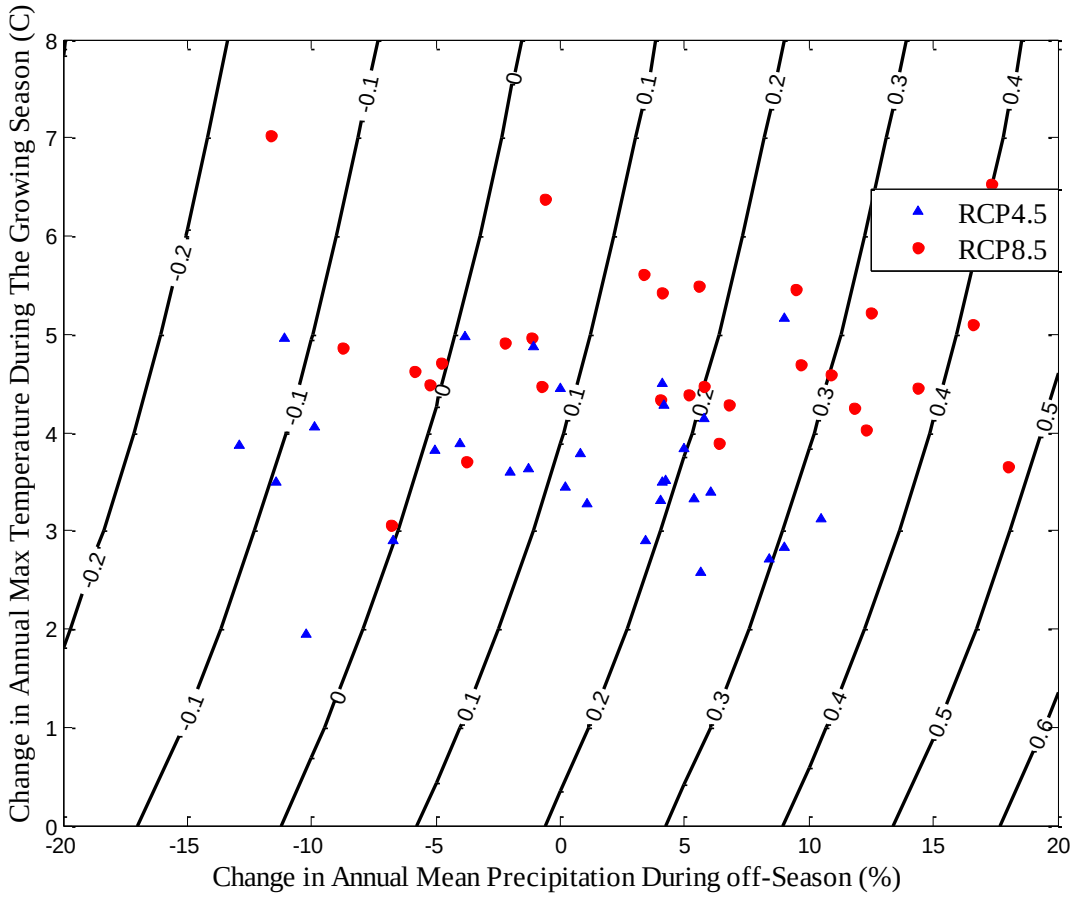

Figure 10. Scatterplot of % change in annual mean precipitation during the off-season and maximum temperature during the growing season, superimposed on the contour lines of I_t for RCP4.5 and RCP8.5 scenarios when P_c is constant at 219.5 mm.

Figure 11 shows the cumulative distribution function of the agricultural water deficit index for the four given time periods compared to the threshold (I_t=0). There are a number of GCM runs below the threshold in all the four time periods. Of the 31 GCMs, there are 6, 10, 5, and 3 GCMs in the periods 2000-2024, 2025-2049, 2050-2074 and 2075-20999, respectively, that predict the basin will have an agricultural water shortage in the corresponding time period. The highest number of GCMs that predict agricultural water shortage is in the period 2025-2049 because, as mentioned before, RCP4.5 assumes

that the greenhouse gas emissions peak around year 2040. The GCMs that predict an average agricultural water shortage over the entire 100 years (2000-2100) are BCC-CSM1.1, CSIRO-MK3.6.0, HADGEM2-AO, and MIROC5. Information on these four GCMs is provided in Table 3. These GCMs have been evaluated and used in many climate studies including the assessment of climate change impacts on water resources (e.g., Lavers et al. 2013; Shiogama et al. 2013; Jiang et al. 2013), indicating their popularity and maybe reliability, too.

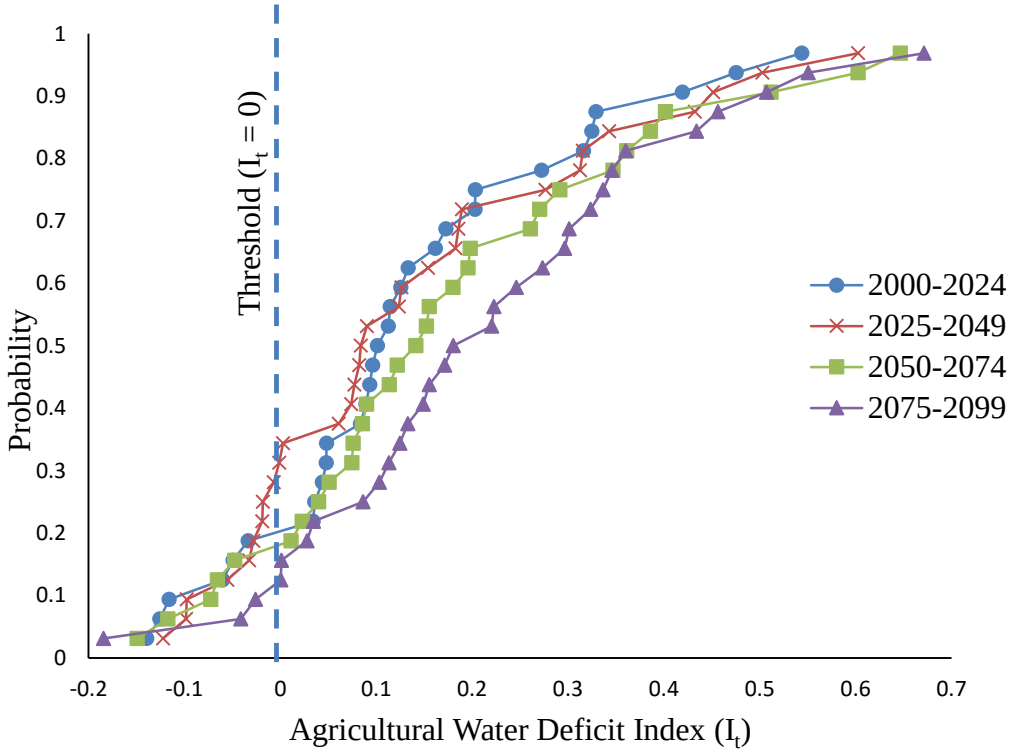

Figure 11. Cumulative distribution function of I_t calculated from GCM projections for the RCP4.5 scenario.

The probability of acceptable and unacceptable water supply scenarios was estimated using the number of GCMs that fall above or below the threshold. Figures 12

and 13 show the probability of acceptable and unacceptable thresholds for both scenarios. For RCP4.5, the probability of unacceptable threshold is 0.19, 0.32, 0.16 and 0.10 for time periods 2000-2024, 2025-2049, 2050-2074 and 2075-2099, respectively. With the RCP8.5 scenario, the probability of unacceptable water supply is 0.17 for the first three time periods and then increased to 0.21 towards the end of the century. The results show a significant risk of agricultural water scarcity for the period 2025-2049 under RCP4.5 and for the period 2075-2099 under the RCP8.5 scenario.

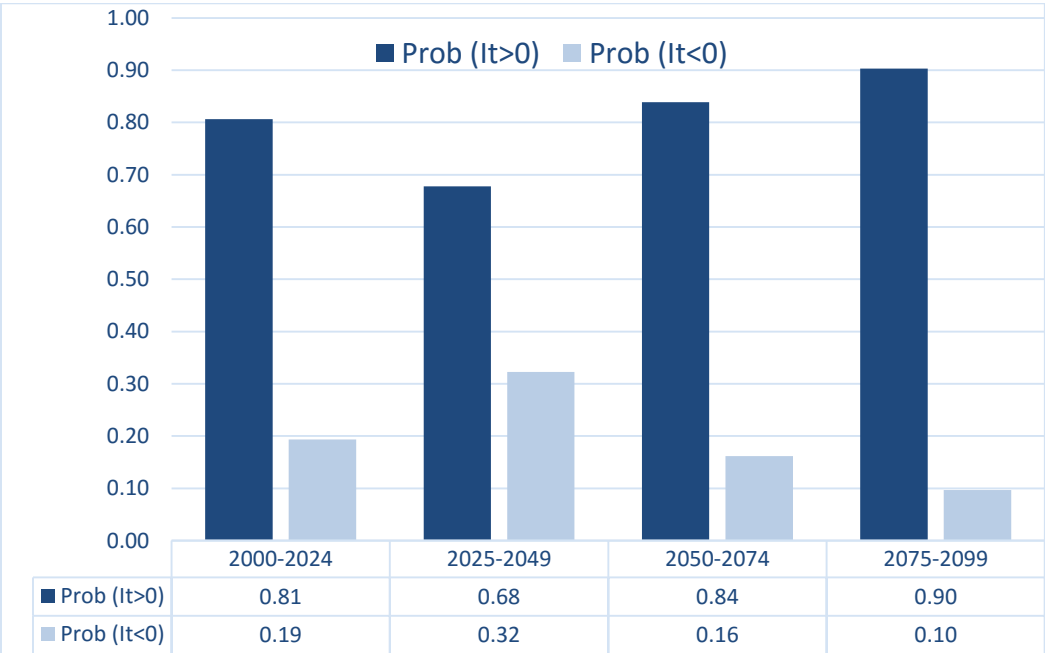

	2000-2024	2025-2049	2050-2074	2075-2099
Prob (It>0)	0.81	0.68	0.84	0.90
Prob (It<0)	0.19	0.32	0.16	0.10

Figure 12. Probability of acceptable and unacceptable water supply scenarios for the RCP4.5 scenario.

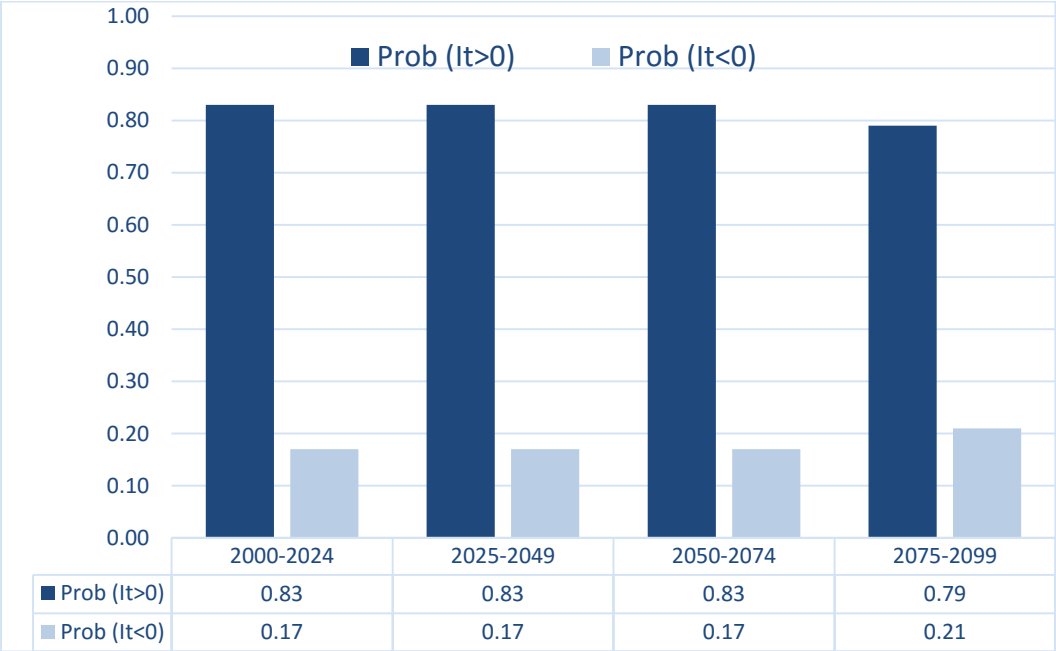

	2000-2024	2025-2049	2050-2074	2075-2099
Prob (It>0)	0.83	0.83	0.83	0.79
Prob (It<0)	0.17	0.17	0.17	0.21

Figure 13. Probability of acceptable and unacceptable water supply scenarios for the RCP8.5 scenario.

4.3 Sensitivity Analysis

There is uncertainty associated with determining the amount of groundwater use for irrigation and the overall irrigation efficiency of the basin. The previous analysis used the values of 2010 across all years and assumed an overall basin-wide irrigation efficiency of 100%. Here overall irrigation efficiency is defined as the ratio of the total amount of water consumed by irrigated crops to the total amount of water diverted from all sources for irrigation. In this section, a sensitivity analysis was conducted to assess the uncertainty associated with these two parameters by varying their values and estimating the corresponding change in the probability of unacceptable water supply.

For groundwater use, we used -20%, -10%, 10% and 20% changes from the 2010 value in the amount of groundwater used for irrigation. This range of values was assumed

based on the variability of groundwater use from historical information. Table 5 shows the probability of unacceptable water supply for the percent change of groundwater use from 2010 for the four given time periods using RCP4.5 and RCP8.5 projections. The probability of unacceptable threshold increases with decreasing used groundwater amount as a result of increasing the agriculture demand deficit. As shown in Table 5, there are no problematic climate conditions (no agricultural water deficit) for all different time periods under both scenarios when the groundwater amount is increased by 20% since the probability of unacceptable threshold is 0. The probability of unacceptable threshold when the groundwater amount is reduced by 20% ranges from 0.52 to 0.74 under both scenarios RCP4.5 and RCP8.5. While the probability of unacceptable threshold when the groundwater amount is reduced by 10% ranges from 0.26 to 0.55 under RCP4.5 and 0.31 to 0.34 under RCP 8.5. When the groundwater amount is increased by 10%, the probability of unacceptable threshold is within 0.03 to 0.10 and 0.03 to 0.17 range under RCP4.5 and RCP 8.5 scenarios, respectively.

Table 5. Probability of unacceptable threshold ($I_t < 0$) for percent changes of groundwater use from 2010 for the given time periods using RCP4.5 and RCP8.5 projections.

		Percent change of groundwater use from 2010			
Scenario	Period	-20%	-10%	10%	20%
RCP4.5	2000-2024	0.71	0.48	0.10	0.00
	2025-2049	0.74	0.55	0.03	0.00
	2050-2074	0.68	0.42	0.06	0.00
	2075-2099	0.52	0.26	0.03	0.00
RCP8.5	2000-2024	0.69	0.31	0.10	0.00
	2025-2049	0.55	0.34	0.03	0.00
	2050-2074	0.55	0.34	0.07	0.00
	2075-2099	0.52	0.31	0.17	0.00

For overall irrigation efficiency, we estimated the probability of unacceptable threshold corresponding to 60%, 70%, and 80% irrigation efficiency. Increasing the overall irrigation efficiency decreases the probability of the problematic climate conditions and having agricultural water shortage. As shown in Table 6, when the overall irrigation efficiency is 60%, there is over 90% probability of an agricultural water deficit in all four time periods. The probability of having an agricultural water shortage for 70% overall irrigation efficiency is over 80% for both scenarios, while the probability of having an agricultural water shortage for 80% overall irrigation efficiency is between 0.55 and 0.83 for both scenarios.

Table 6. Probability of unacceptable threshold ($I_t < 0$) for different irrigation efficiencies using RCP4.5 and RCP8.5 projections.

		Overall Irrigation Efficiency		
Scenario	Period	60%	70%	80%
RCP4.5	2000-2024	1.00	0.94	0.77
	2025-2049	1.00	0.87	0.74
	2050-2074	1.00	0.90	0.68
	2075-2099	0.97	0.84	0.61
RCP8.5	2000-2024	1.00	0.93	0.83
	2025-2049	1.00	0.83	0.62
	2050-2074	0.93	0.79	0.59
	2075-2099	0.90	0.69	0.55

From previous studies (Barta 2004; NRCS 2006), the overall irrigation efficiency was estimated to be approximately 60% for the Sevier River Basin. As shown in the results, overall irrigation efficiency and the amount of groundwater used for irrigation are

crucial factors that affect agricultural water shortage in the basin. Therefore, efficient management of these two factors is important to sustain the agricultural economy in the basin. It is shown in Table 6 that 60 % overall irrigation efficiency will lead to agricultural water shortage in the basin for all time periods. In managing water in a semi-arid region such as the Sevier River Basin, these results suggest that irrigation efficiency and groundwater use play important roles. Therefore, ongoing and future monitoring and data gathering should emphasis the importance of these parameters.

CHAPTER 5

5. SUMMARY AND CONCLUSIONS

Water resources management plays an important role in the social and economic development of semi-arid areas, especially in sustaining agricultural productivity. The major challenge that water managers face in semi-arid regions is water scarcity. Semi-arid regions already face water scarcity and there are many factors that may make the situation worse in the future. Climate change is one of those major stresses that can affect water supply and therefore affect rural livelihood in majority of river basins.

In this study, a bottom-up decision scaling approach was used for risk assessment of climate change impacts. The approach was used to explore the risk of an agricultural water deficit in a semi-arid and snowmelt dominated basin under climate change. The bottom-up decision scaling approach links a stochastic analysis with the use of climate change projections. This approach is innovative because, unlike traditional approaches, it uses GCM projections in the final stage. The approach begins using a vulnerability analysis to identify the system sensitivity to climate change; then it uses GCM projections to predict water scarcity scenarios based on a water deficit index proposed in this study. GCM predictions that produce water scarcity scenarios are used to calculate the risk of water scarcity under climate change. The advantage of this approach is that it is able to accommodate a large number of GCM projections without conducting individual analyses for each projection, as is in the case in the top-down approach. The Sevier River Basin in south central Utah was used as a case study to demonstrate the

approach. An agricultural water deficit index was developed to evaluate the basin performance in terms of the water supply to meet the agricultural demand. A stochastic simulation was used in the vulnerability analysis to identify sensitivity to climate change. The basin climate response function was developed using a multilinear regression model. Finally, downscaled and bias-corrected GCM projections of precipitation and temperature for the period 2000-2099 were used as inputs to the climate response function to estimate the risk probability of not having enough water supply to meet the future agricultural demand.

The results indicated that the Sevier River Basin's performance in the terms of agricultural water shortage is more sensitive to off-season precipitation change than to growing season precipitation and annual maximum growing season temperature change. The projections of temperature and precipitation in the basin showed an increasing trend for temperature, but does not show a similar trend for precipitation. It was found that there is a significant risk probability of having agricultural water shortage in the period 2025-2049 under RCP4.5 and 2075-2099 under RCP8.5 scenarios. These results suggest that climate change adaptation strategies may be required to face these challenges. The results demonstrated that groundwater use in irrigation and irrigation efficiency have a significant impact on risk probability of having agricultural water shortage in the future. The bottom-up decision scaling approach used in this research shows good performance in exploring the risks of agricultural water shortage in a semi-arid and snowmelt-dominated basin under present and future climate conditions.

REFERENCES

Anderson, E. A. (1976). “A point energy and mass balance model of a snow cover.” Technical Report NWS 19, National Oceanic and Atmospheric Administration (NOAA), US Department of Commerce, Silver Spring, MD US.

Araya, A., Habtu, S., Hadgu, K. M., Kebede, A., and Dejene, T. (2010). “Test of AquaCrop model in simulating biomass and yield of water deficient and irrigated barley (Hordeum vulgare).” Agricultural Water Management, 97(11), 1838-1846.

Barta, R., Broner, I., and Schneekloth, J. (2004). “Colorado High Plains Irrigation Practices Guide.” Special Report No. 14, Colorado Water Resources Research Institute, Fort Collins, Colorado.

Brissette, F. P., Khalili, M., and Leconte, R. (2007). “Efficient stochastic generation of multi-site synthetic precipitation data.” Journal of Hydrology,345(3), 121-133.

Brown, C., Ghile, Y., Laverty, M., and Li, K. (2012). “Decision scaling: Linking bottom-up vulnerability analysis with climate projections in the water sector.” Water Resources Research Water Resour. Res., 48(9).

Christensen, N., and Lettenmaier, D. P. (2006). “A multimodel ensemble approach to assessment of climate change impacts on the hydrology and water resources of the Colorado River Basin.” Hydrology and Earth System Sciences Discussions, 3(6), 3727-3770.

Cooper, V. A., Nguyen, V. T. V., and Nicell, J. A. (2007). “Calibration of conceptual rainfall–runoff models using global optimisation methods with hydrologic process-based parameter constraints.” Journal of Hydrology,334(3), 455-466.

Doesken, N. J., and Judson, A. (1997). “The Snow Booklet: A Guide to the Science, Climatology, and Measurement of Snow in the United States.” Department of Atmospheric Science, Colorado State University, Colorado.

Döll, P. (2002). “Impact of Climate Change and Variability on Irrigation Requirements: A Global Perspective.” Climatic Change, 54(3), 269–293.

FAOWATER (2015). “Water Scarcity.” <http://www.fao.org/nr/water/topics_scarcity.html> (July, 2016).

Fischer, G., Tubiello, F. N., Velthuizen, H. V., and Wiberg, D. A. (2007). "Climate change impacts on irrigation water requirements: Effects of mitigation, 1990–2080." Technological Forecasting and Social Change, 74(7), 1083–1107.

García, L. E., Matthews, J. H., Rodriguez, D. J., Wijnen, M., DiFrancesco, K. N., and Ray, P. (2015). "Beyond downscaling: a bottom-up approach to climate adaptation for water resources management." AGWA Report 01, The World Bank, Washington DC.

Ghile, Y. B., Taner, M. Ü., Brown, C., Grijsen, J. G., and Talbi, A. (2014). "Bottom-up climate risk assessment of infrastructure investment in the Niger River Basin." Climatic change, 122(1-2), 97-110.

Gondim, R. S., Castro, M. A. D., Maia, A. D. H., Evangelista, S. R., and Fuck, S. C. D. F. (2012). "Climate Change Impacts on Irrigation Water Needs in the jaguaribe River Basin." JAWRA Journal of the American Water Resources Association, 48(2), 355–365.

Gourbesville, P. (2008). "Challenges for integrated water resources management." Physics and Chemistry of the Earth, Parts A/B/C, 33(5), 284-289.

He, C., and Zhou, T. (2015). "Responses of the western North Pacific Subtropical High to global warming under RCP4. 5 and RCP8. 5 scenarios projected by 33 CMIP5 models: the dominance of tropical Indian Ocean–tropical western Pacific SST gradient." Journal of Climate, 28(1), 365-380.

IPCC. (1995). "Water Resources Management. Scientific-Technical Analyses of Impacts, Adaptations, and Mitigation of Climate Change." Contribution of Working Group II to the Second Assessment Report of the Intergovernmental Panel on Climate Change, Intergovernmental Panel on Climate Change, Geneva.

IPCC. (2007). "Observations: Surface and Atmospheric Climate Change, The Physical Science Basis." Contribution of Working Group I to the Fourth Assessment Report of the Intergovernmental Panel on Climate Change, Intergovernmental Panel on Climate Change, Geneva.

Jiang, D., and Tian, Z. (2013). "East Asian monsoon change for the 21st century: Results of CMIP3 and CMIP5 models." Chinese Science Bulletin, 58(12), 1427-1435.

Keller, D. E., Fischer, A. M., Frei, C., Liniger, M. A., Appenzeller, C., and Knutti, R. (2015). “Implementation and validation of a Wilks-type multi-site daily precipitation generator over a typical Alpine river catchment.” Hydrol. Earth Syst. Sci. Hydrology and Earth System Sciences, 19(5), 2163–2177.

Kim, D., and Kaluarachchi, J. J. (2016). “A risk-based hydro-economic analysis for land and water management in water deficit and salinity affected farming regions.” Agricultural Water Management, 166, 111-122.

Kim, D., and Kaluarachchi, J. (2014). “Predicting streamflows in snowmelt-driven watersheds using the flow duration curve method.” Hydrol. Earth Syst. Sci. Hydrology and Earth System Sciences, 18(5), 1679–1693.

Kim, D., and Kaluarachchi, J. (2015). “Validating FAO AquaCrop using Landsat images and regional crop information.” Agricultural Water Management, 149, 143–155.

Lavers, D. A., Allan, R. P., Villarini, G., Lloyd-Hughes, B., Brayshaw, D. J., and Wade, A. J. (2013). “Future changes in atmospheric rivers and their implications for winter flooding in Britain.” Environmental Research Letters, 8(3), 034010.

Li, K., Qi, J., Brown, C., and Ryan, J. (2014). “Effect of scenario assumptions on climate change risk estimates in a water resource system.” Climate Research, 59(2), 149-160.

Llewellyn, D., and Vaddey, S. (2013). “West-wide Climate Risk Assessment: Upper Rio Grande Impact Assessment.” US Department of the Interior, Bureau of Reclamation, Upper Colorado Region, Albuquerque Area Office.

Mainuddin, M., Kirby, M., Chowdhury, R. A. R., and Shah-Newaz, S. M. (2014). “Spatial and temporal variations of, and the impact of climate change on, the dry season crop irrigation requirements in Bangladesh.” Irrig Sci Irrigation Science, 33(2), 107–120.

Masoner, J. R., Mladinich, C. S., Konduris, A. M., and Smith, S. J. (2003). “Comparison of irrigation water use estimates calculated from remotely sensed irrigated acres and state reported irrigated acres in the Lake Altus drainage basin, Oklahoma and Texas, 2000 growing season.” Water-Resources Investigations Report, 03-4155, US Geological Survey, USGS, Colorado.

Maurer, E. P., Brekke, L., Pruitt, T., and Duffy, P. B. (2007). “Fine-resolution climate projections enhance regional climate change impact studies.” Eos, Transactions American Geophysical Union, 88(47), 504-504.

Middelkoop, H., Daamen, K., Gellens, D., Grabs, W., Kwadijk, J.C., Lang, H., Parmet, B.W., Schädler, B., Schulla, J. and Wilke, K., 2001. "Impact of climate change on hydrological regimes and water resources management in the Rhine basin." Climatic change, 49(1-2), 105-128.

NRCS (2006). "Rapid Watershed Assessment - HUC # 16030005 Lower Sevier River - Millard/Juab Counties, Utah." Natural Resources Conservation Service, Utah.

Qian, B., Corte-Real, J., and Xu, H. (2002). "Multisite stochastic weather models for impact studies." International Journal of climatology, 22(11), 1377-1397.

Reclamation. (2014). "Downscaled CMIP3 and CMIP5 Climate and Hydrology Projections: Release of Hydrology Projections, Comparison with preceding Information, and Summary of User Needs." U.S. Department of the Interior, Bureau of Reclamation, Technical Services Center, Denver, Colorado.

Seager, R., Ting, M., Held, I., Kushnir, Y., Lu, J., Vecchi, G., Huang, H.P., Harnik, N., Leetmaa, A., Lau, N.C. and Li, C. (2007). "Model projections of an imminent transition to a more arid climate in southwestern North America." Science, 316(5828), 1181-1184.

Shiogama, H., Watanabe, M., Imada, Y., Mori, M., Ishii, M., and Kimoto, M. (2013). "An event attribution of the 2010 drought in the South Amazon region using the MIROC5 model." Atmospheric Science Letters, 14(3), 170-175.

Sivakumar, M. V. K., Das, H. P., and Brunini, O. (2005). "Impacts of Present and Future Climate Variability and Change on Agriculture and Forestry in the Arid and Semi-Arid Tropics." Climatic Change, 70(1-2), 31-72.

Snover, A. K., Hamlet, A. F., and Lettenmaier, D. P. (2003). "Climate-change scenarios for water planning studies: Pilot applications in the Pacific Northwest." Bulletin of the American Meteorological Society, 84(11), 1513.

Srikanthan, R., and Pegram, G. G. (2009). "A nested multisite daily rainfall stochastic generation model." Journal of Hydrology, 371(1), 142-153.

Steduto, P., Hsiao, T. C., Raes, D., and Fereres, E. (2009). "AquaCrop—The FAO crop model to simulate yield response to water: I. Concepts and underlying principles." Agronomy Journal, 101(3), 426-437.

Stöckle, C. O., Nelson, R. L., Higgins, S., Brunner, J., Grove, G., Boydston, R., Whiting, M., and Kruger, C. (2010). "Assessment of climate change impact on Eastern Washington agriculture." Climatic Change, 102(1-2), 77–102.

Stricevic, R., Cosic, M., Djurovic, N., Pejic, B., and Maksimovic, L. (2011). "Assessment of the FAO AquaCrop model in the simulation of rainfed and supplementally irrigated maize, sugar beet and sunflower." Agricultural water management, 98(10), 1615-1621.

Vano, J. A., Scott, M. J., Voisin, N., Stöckle, C. O., Hamlet, A. F., Mickelson, K. E. B., Elsner, M. M., and Lettenmaier, D. P. (2010). "Climate change impacts on water management and irrigated agriculture in the Yakima River Basin, Washington, USA." Climatic Change, 102(1-2), 287–317.

Vanuytrecht, E., Raes, D., and Willems, P. (2014). "Global sensitivity analysis of yield output from the water productivity model." Environmental Modelling and Software, 51, 323-332.

Wilks, D. (1999). "Simultaneous stochastic simulation of daily precipitation, temperature and solar radiation at multiple sites in complex terrain." Agricultural and Forest Meteorology, 96(1-3), 85–101.

Wilks, D. S. (1995). Statistical methods in the atmospheric sciences (Vol. 100), Academic press, Elsevier, Oxford.

Yan, D., Werners, S. E., Ludwig, F., and Huang, H. Q. (2015). "Hydrological response to climate change: The Pearl River, China under different RCP scenarios." Journal of Hydrology: Regional Studies, 4, 228-245.

Zhang, Y., You, Q., Chen, C., and Ge, J. (2016). "Impacts of climate change on streamflows under RCP scenarios: A case study in Xin River Basin, China." Atmospheric Research, 178, 521-534.